Pergamon

Bioorganic & Medicinal Chemistry, Vol. 3, No. 11, pp. 1465–1477, 1995

0968-0896/95 $9.50 + .00

0968-0896(95)00131-X

Molecular Dynamics Simulations of m3-Muscarinic Receptor Activation and QSAR Analysis

Francesca Fanelli, M. Cristina Menziani and Pier G. De Benedetti*
Dipartimento di Chimica, Università di Modena, via Campi 183, 41100 Modena, Italy

Abstract—Molecular dynamics simulations of the rat m3-muscarinic seven-helix-bundle receptor models were performed on the free, agonist-bound and antagonist-bound forms. A comparative structural/dynamics analysis was performed in order to explain the perturbations induced by the functionally different ligands when binding to their target receptor. Theoretical quantitative structure–activity relationship models were developed; a good correlation was obtained between the interaction energies of the minimized average ligand–receptor complexes and the pharmacological affinities of the considered ligands. The consistency obtained between the structural rearrangement of the transmembrane seven-helix-bundle models considered and the experimental pharmacological efficacies and affinities of the ligands constitutes an important validation of the 3-D models proposed and allows the inference of the mechanism of ligand-induced or mutation-induced receptor activation at the molecular level.

Introduction

G-Protein coupled receptors (GPCRs) constitute a superfamily of proteins that transduce signals across the cell membrane by receiving a ligand (or a photon in the case of opsins) at the external side and by activating a G-protein at the cytosolic side.

Several hypotheses on the signal transduction mechanism, at the molecular level, have been carried out.[1-3] Receptor-activation models obtained by combining three-dimensional (3-D) molecular models of receptor structures and computational simulations of receptor dynamics have also been elaborated.[4-6] In this context, we have recently presented the results of a comparative molecular dynamics (MD) study on the seven-helix-bundle models of the hamster α_{1B}-adrenergic receptor (AR) and of the rat m3-muscarinic receptor in their free, agonist-bound and antagonist-bound forms.[7] Moreover, three mutant forms of the m3- muscarinic receptor: N617(507) → A (the numbering is arbitrary: the first digit corresponds to the helix and the next two digits indicate the position of the residue in the helix; in parenthesis the standard numbering for the amino acids in receptor sequences is reported), N617(507) → D and the N617(507) → S have also been simulated;[7] among these, the N617(507) → S mutant shows a constitutive activity.[8]

We found that the structural modifications induced by the agonist *R*-(–)-norepinephrine and by the antagonist prazosin on the starting average-minimized structure of the free α_{1B}-AR are consistent with the modifications induced by the agonist carbachol and by the antagonist *N*-methylscopolamine (NMS) on the m3-muscarinic receptor. In fact, both considered antagonists substantially preserve the average topography of the H-bonding interactions which involve, in the free receptor form, the amino acids of the highly conserved polar pocket lying near the cytosolic side and formed by N119(85), D210(113), R325(165), N717(539) and Y721(543).

To the contrary, the agonists *R*-(–)-norepinephrine and carbachol induce an evident perturbation in the distribution of the conformer population observed during the MD simulation of their target receptor, resulting in a rearrangement of the highly conserved polar pocket, characterized also by the 'shift out' of R325(165). We observed that this arginine in the free and antagonist-bound forms makes persistent H-bonds with N119(85), while in the agonist-bound form shifts out from the pocket by losing the interaction with N119(85). Moreover, we observed that the shift of R325(165) is also induced by mutating N617(507) into a serine residue, consistently with the experimental observation that this mutation activates the m3 receptor.[8] Site-directed mutagenesis experiments have shown that this arginine, which is part of the highly conserved DRY sequence, has an essential functional role in GPCRs.[9,10]

The results obtained prompted us to extend the MD study to a larger series of ligands. This work presents the results of the MD study carried out on the seven-helix-bundle of the rat m3-muscarinic receptor complexed with the agonists and the antagonists reported in Scheme 1. A comparative analysis of the structural/dynamics perturbations induced by the functionally different ligands (agonists and antagonists) upon the binding to the average structure of their target receptor have been performed. Moreover, theoretical quantitative structure–activity relationship (QSAR) analysis has been carried out by correlating the computed interaction energies of the minimized average ligand–receptor complexes with the pharmacological affinities.[8]

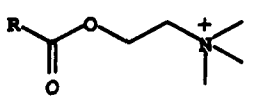

1 ACETYLCHOLINE : R = CH3
2 CARBACHOL: R = NH2

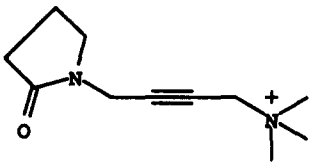

3 OXOTREMORINE-M

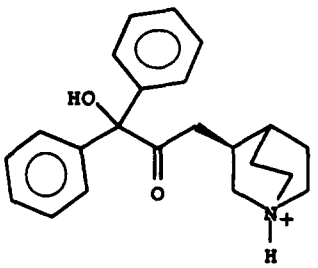

4 (-)-QUINUCLIDINYL BENZILATE ((-)-QNB)

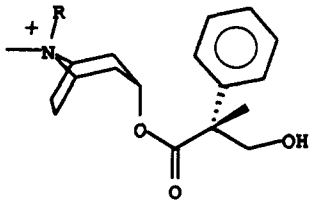

5 ATROPINE: R = H
6 N-METHYLATROPINE : R = CH_3

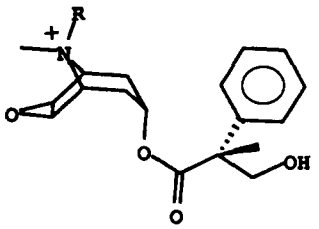

7 (-)-SCOPOLAMINE: R = H
8 (-)-N-METHYLSCOPOLAMINE ((-)-NMS): R = CH_3

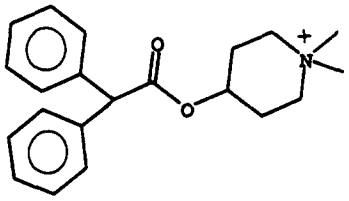

9 4-DAMP

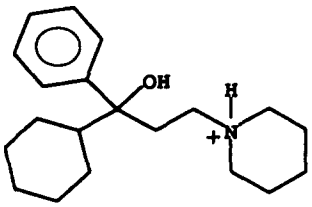

10 TRIHEXYPHENIDYL

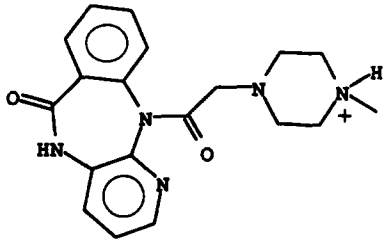

11 PIRENZEPINE

Scheme 1.

Results and Discussion

Ligand–m3 muscarinic receptor dynamics models

Figure 1 shows the minimized average structure of the m3-muscarinic receptor. Only the amino acid side chains more conserved in the GPCRs, or shown to be important for ligand binding or for receptor activation are reported in this figure; they are numbered following the arbitrary criteria.

The effects of the antagonist and the agonist binding on the structural features of the free m3-muscarinic receptor model were studied by analyzing the persistence of the H-bonding interactions which involve the most conserved polar amino acids during the last 100 picoseconds (ps) time period of each MD simulation. In this respect, Table 1 shows the conserved polar amino acid pairs which are involved in H-bonding interactions in more than 50% of the structure collected; the H-bonding interactions listed in this Table are mainly persistent during the equilibrated time period of the MD simulations. Only the interhelical interactions between the amino acid side chains are reported in Table 1. Furthermore, the data regarding the free, the NMS-bound and carbachol-bound forms, presented in the previous paper,[7] have also been inserted for comparative purposes.

From this Table it emerges that the distribution of the

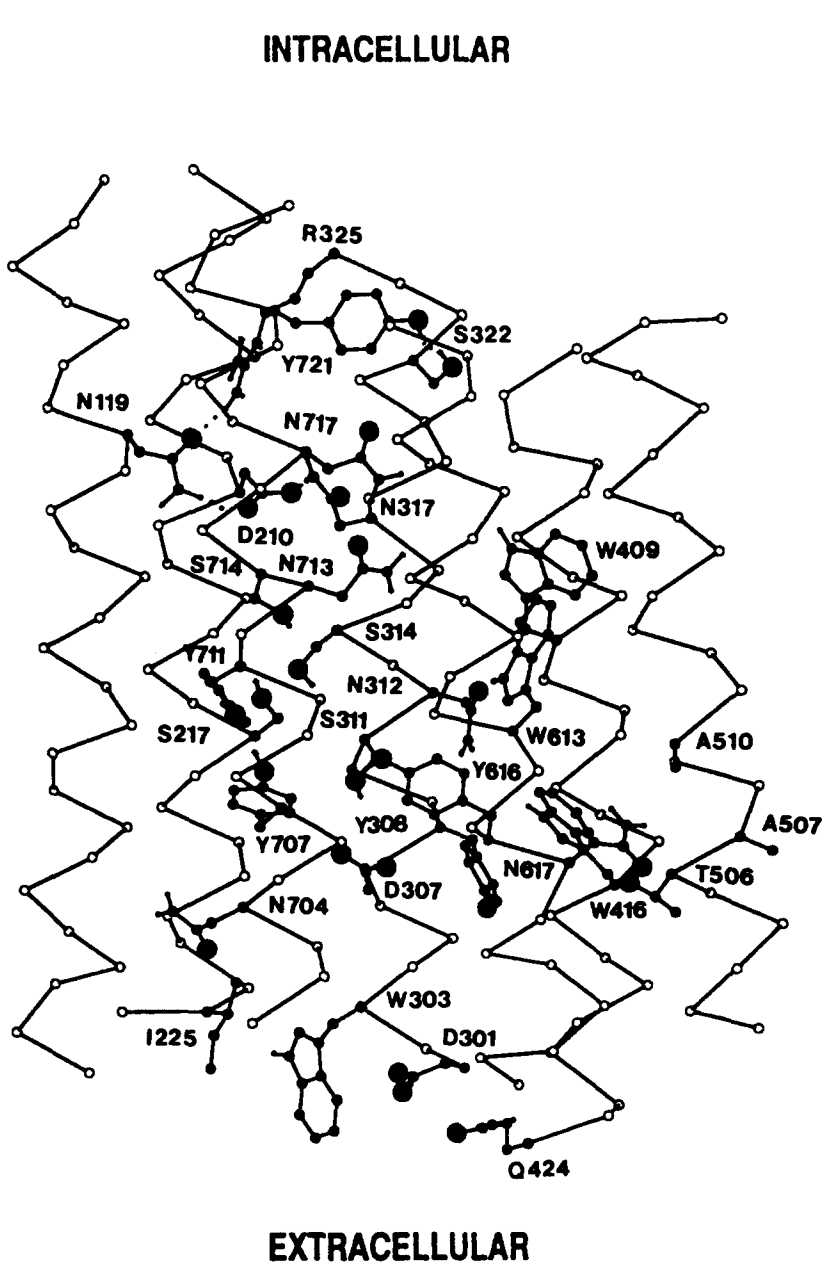

Figure 1. Side view of the minimized average structure of the m3-muscarinic receptor-free form, in a direction perpendicular to the main axes of the seven α-helices. Only the amino acid side chains more conserved in the GPCRs or shown to be important for ligand binding or for receptor activation are reported and labelled according to the arbitrary numbering.

amino acid pairs which make permanent H-bonds in the receptor-free and antagonist-bound forms is similar. The differences mainly concern the amino acid pairs which are directly involved in the antagonist binding, such as S217(120), D307(147), S314(154) and Y711(533). As for the highly conserved polar pocket, H-bonding interactions mainly involve the amino acid pairs N119(85)–D210(113), N119(85)–R325(165) and D210(113)–N317(157) in both the free and antagonist-bound receptor forms. Additional H-bonding interactions are observed between D210(113) and R325(165) in the m3 complexed with *N*-methylatropine (**6**), (–)-scopolamine (**7**), (–)-NMS (**8**), DAMP (**9**), trihexyphenidyl (**10**) and pirenzepine (**11**). The S322(162)–Y721(543) interaction observed in the free receptor form is conserved only in the *N*-methylatropine (**6**) and in the NMS-bound (**8**) forms and is replaced by the S322(162)–N717(539) interacting pair in the other antagonist–m3 receptor dynamic models.

The agonist binding induces perturbations in the average H-bonding interaction pattern which is found in the receptor-free form. This is due to the fact that the agonists interact directly with some residues which are involved in interhelical interactions in the receptor-free form, such as D307(147), S311(151), T506(234) and Y616(506), and induce structural changes in the highly conserved polar pocket closed to the intracellular side of the receptor notwithstanding the binding domain is

Table 1. Conserved polar amino acid pairs involved in persistent H-bonding interactions during the molecular dynamic simulation of the free, agonist-bound and antagonist-bound forms of the rat m3-muscarinic receptor.

	T106	T115	N119	D210	S217	D307	Y308	S311	N312	S314	N317	S322	R325	W416	T506	W613	Y616	N617	Y711	S714	N717	Y721
m3			D210 R325	N119 N317	S314 Y711	Y616		Y616	W613	S217 Y711	D210	Y721	N119		N617	N312	D307 S311	T506	S217 S314			S322
AGONISTS																						
m3-ACETYLCHOLINE			D210	N119 N317	S314		Y616			S217 Y711	D210						Y308		S314			
m3-CARBACHOL			D210 S714	N119 N317 S714	S314 Y711		Y616			S217 Y711	D210						Y308		S217 S314	D210		
m3-OXOTREMORINE-M			D210	N119 N317	S314 Y711		Y616			S217 Y711	D210	N717			N617		Y308	T506	S217 S314		S322	
ANTAGONISTS																						
m3-(-)-QNB		D210	D210 R325	T115 N119 N317	Y711	Y616		Y616	W416 W613		D210	N717	N119	N312	N617	N312	D307 S311	T506	S217		S322	
m3-ATROPINE			D210 R325	N119 N317				Y616	W613		D210	N717	N119		N617	N312	S311	T506			S322	
m3-N-METHYLATROPINE			D210 R325	N119 R325				Y616				N717 Y721	N119 D210				S311				S322	S322
m3-(-)-SCOPOLAMINE		D210	D210 R325	T115 N119 N317 R325				Y616	W416		D210	N717	N119 D210	N312			S311				S322	
m3-(-)-NMS			D210 R325	N119 N317 R325		Y616		Y616	W613		D210	Y721	N119 D210		N617	N312	D307 S311	T506				S322
m3-4-DAMP	Y711		D210 R325	N119 N317 R325	S314	Y616		Y616	W613	S217	D210	N717	N119 D210		N617	N312	D307 S311	T506	T106		S322	
m3-TRIHEXYLPHENIDYL			D210 R325	N119 N317 R325	Y711			Y616			D210		N119 D210		N617		S311	T506	S217	D210		
m3-PIRENZEPINE			R325	N317 R325	Y711	Y616		Y616		S714	D210	N717	N119 D210		N617		D307 S311	T506	S217	S314	S322	

close to the extracellular side (Fig. 3). In this context, N119(85) loses the interaction with R325(165) upon the agonist binding; moreover, S322(162) loses the interaction with Y721(543) in all the agonist-bound forms and makes H-bonding interactions with N717(539) in the oxotremorine-M–receptor complex.

Figure 2 allows a visualization of the average topography of the H-bonding interactions involving the amino acids of the highly conserved polar pocket. In this figure, the amino acid side chains have been extracted from each minimized average ligand–receptor complexes. These interactions are persistent during the MD simulation time period.

It can be seen that the charge reinforced H-bonding interactions between R325(165) and N119(85) is shared by the receptor-free and by all the antagonist–receptor complexes and is broken by the agonist binding. This interaction which characterizes a functional class of ligands may be connected with the receptor activation mechanism (Fig. 2).

The agonist-induced rearrangements of the highly conserved polar pocket are also caused by the movements of the helices 3–7 (rms deviations of the backbone α-carbon atoms of helices 3–7 with respect to the free receptor structure are about 2 Å while rms deviations of the helix 1–3 α-carbon atoms are about 1 Å). It is worth noting that both helices 5 and 6 contain a highly conserved proline near the agonist binding site; these prolines are able to induce kinks into the helices and may contribute to the receptor-activation mechanism. To the contrary, the antagonists induced struct-

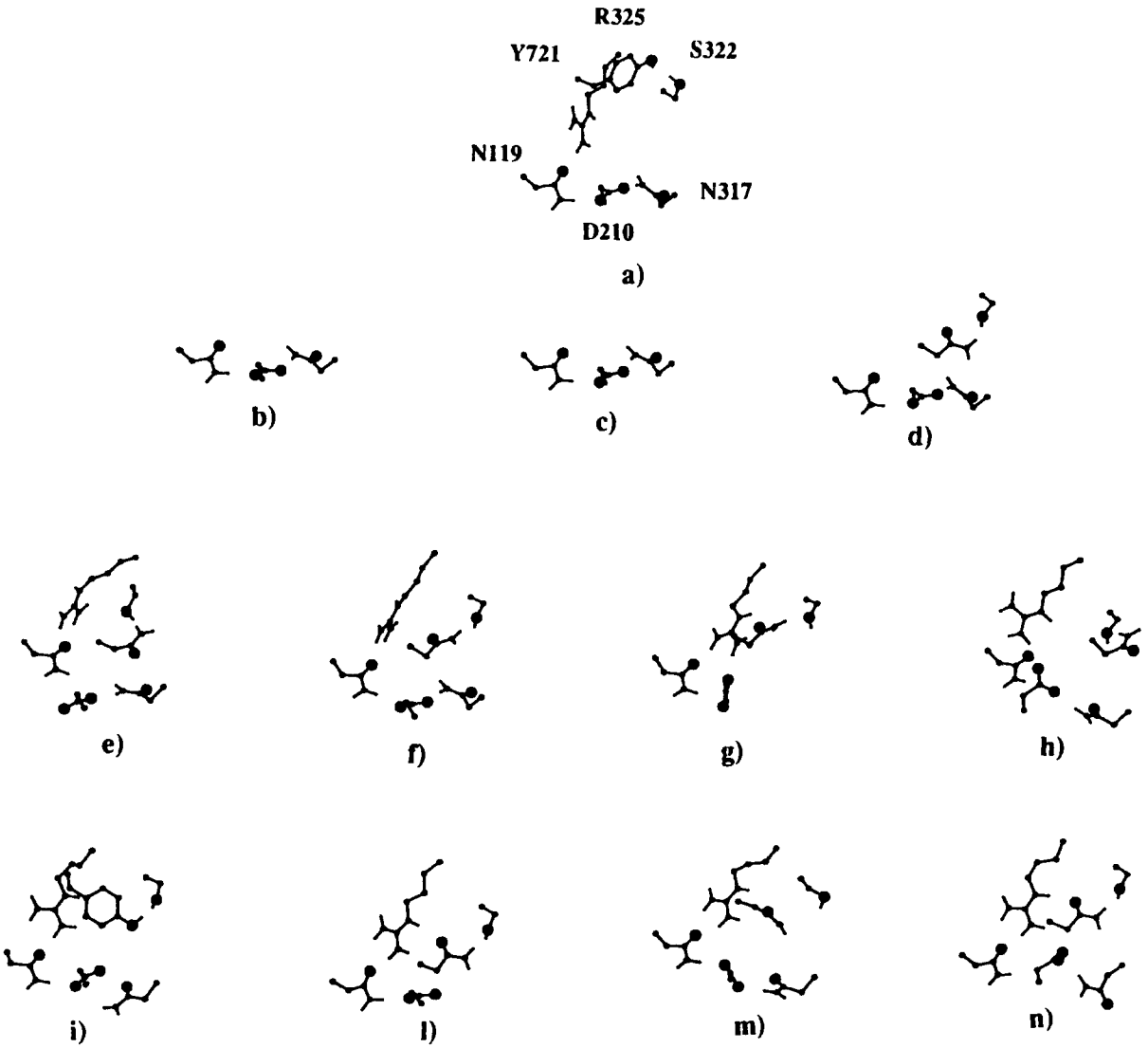

Figure 2. Amino acid side chains of the highly conserved polar pocket extracted from the minimized average structures of the m3-muscarinic receptor in the a) free, b) acetylcholine-, c) carbachol-, d) oxotremorine-M e) (–)-QNB-, f) atropine-, g) *N*-methylatropine-, h) scopolamine-, i) NMS-, l) 4-DAMP, m) trihexyphenidyl and n) pirenzepine-bound forms. Only the amino acids involved in H-bonding interactions which persistently occur during the molecular dynamics simulation time period are reported in this figure. The amino acids are labelled according to the arbitrary numbering.

ural changes mainly involving helices 1–3 (rms deviations of the helix 1–3 α-carbon atoms with respect to the free receptor structure are about 2 Å) (Fig. 4).

Theoretical QSAR models and mechanistic interpretation of the dynamic structural rearrangement of the receptor upon the agonist and the antagonist binding

The consistency obtained between the time-dependent structural rearrangement of the transmembrane seven-helix-bundle models considered and the experimental pharmacological efficacies of the ligands constitutes a good validation of the 3-D models obtained.[11]

Interestingly, the total interaction energies (IE) of the minimized average structures of the ligand–receptor complexes give good linear correlations with the pharmacological affinities (Table 2 and Fig. 5), notwithstanding the very different structural features of the considered ligands. This fact raises the problem of the role of the entropic terms in correlating measured relative free energies (pK_i) with calculated interaction enthalpies (IE). The entropic terms cannot be considered negligible (or equal) for the considered ligands but they are assumed to be linearly related to the enthalpic terms with a negative slope (compensative effects), as recently shown by the analysis of a large set of binding thermodynamic data available for membrane neuronal receptors systems.[12]

The energy contribution of the amino acids which give persistent interactions with the ligands during the MD simulation are listed in Table 2; only the energy values below –1 kcal mol^{-1} have been considered.

The binding of the agonists mainly consists of specific interactions.[13] In fact, during the last 100 ps of the MD

Figure 3. Side view of the minimized average structure of the m3-muscarinic receptor in the free, atropine-bound and acetylcholine-bound forms, in a direction perpendicular to the main axes of the seven α-helices. Only the amino acid side chains of the highly conserved polar pocket lying near the intracellular side are reported. The selected colours are blue, orange, green, pink, yellow, light blue and violet for helices 1–7, respectively. The amino acid side chains of the highly conserved polar pocket are represented in white.

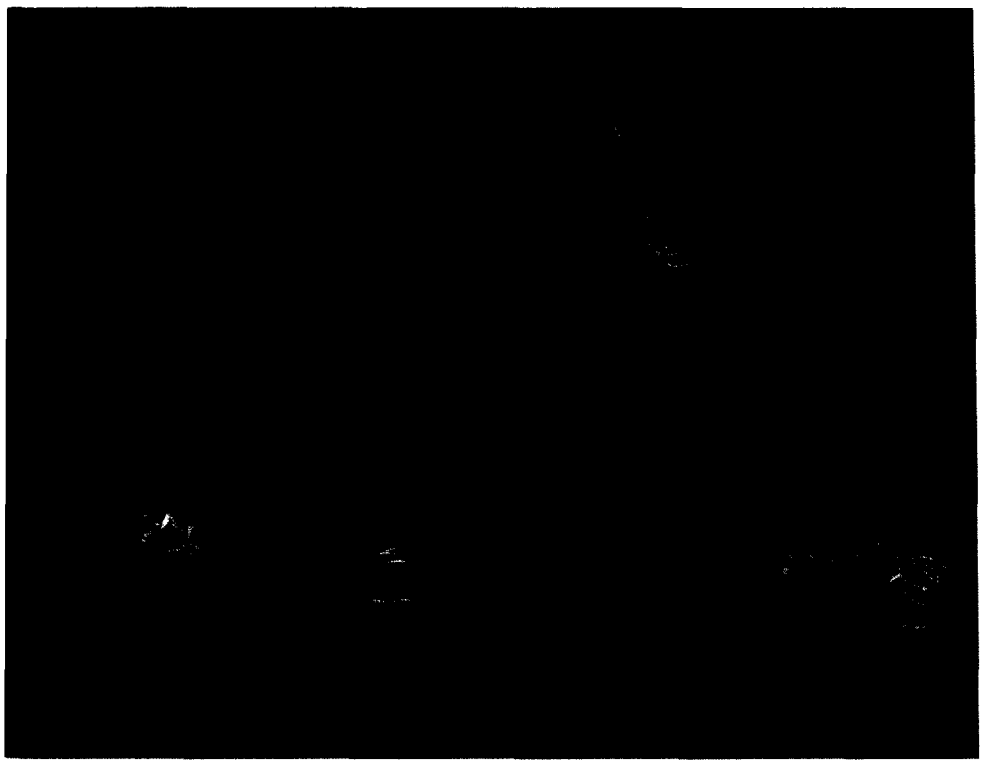

Figure 4. Side view of the minimized average structure of the m3-muscarinic receptor in the free, NMS-bound and carbachol-bound forms, in a direction parallel to the main axes of the seven α-helices. The selected colours are blue, orange, green, pink, yellow, light blue and violet for helices 1–7, respectively.

Table 2. Experimental binding affinities (pK_i), computed total interaction energies of the minimized average ligand-receptor complexes (IE, kcal mol^{-1}) and energy contribution (kcal mol^{-1}) to the total IE of the amino acid residues interacting with the ligands considered.

N.	pKi[a]	IE	I104	L107	T108	L111	T115	D210	I213	S217	M218	L220	F221	T223	Y224	I225	W303	L304	I306
1	5.72	-48.97																-4.73	
2	4.82	-47.47																-3.13	
3	5.72	-51.04																-2.55	
4	10.51	-76.26		-2.06	-12.37	-1.02				-6.51		-3.58	-4.72		-1.00	-2.12	-1.03		-3.02
5	9.70	-77.29				-1.23				-8.80	-2.30	-2.20	-3.14						-1.98
6	10.02	-74.91						-2.71	-2.76	-8.46		-2.31	-3.22		-2.23				
7	10.96	-77.63					-1.01			-7.98		-2.34	-3.29		-1.54				-1.30
8	10.42	-77.67				-3.54	-2.77	-1.56		-7.35	-3.18		-2.30						
9	9.79	-73.75			-1.69	-1.47	-1.92	-2.67		-8.84	-5.20		-2.03						
10	8.70	-68.66								-1.82		-1.80	-4.48		-1.20	-1.91	-1.57		
11	6.78	-62.80	-2.64		-3.62							-5.73	-1.67	-2.35	-6.45		-5.93		-6.23

N.	D307	Y308	A310	S311	S314	L318	I420	T506	Y616	M619	V620	Y702	W703	N704	Y707	C710	Y711	S714
1	-5.11	-6.17					-1.95	-7.48	-10.79		-1.65							
2	-5.71	-4.89					-1.52	-7.44	-11.26		-2.35							
3	-5.89	-5.03		-1.80			-1.92	-6.21	-7.00	-2.08	-2.70				-1.68			
4	-14.97		-2.17	-1.51					-1.16						-5.55		-4.25	
5	-14.05		-2.00	-8.11	-5.00								-3.64		-6.96	-1.51	-3.74	
6	-7.03		-2.68	-3.43	-13.80	-1.31									-3.34	-1.86	-4.77	-1.28
7	-14.21		-2.58	-8.90	-6.16								-3.11		-6.76	-2.71	-1.62	
8	-8.24		-2.16	-2.59	-8.56	-1.27			-1.69						-6.59	-2.10	-1.11	-7.80
9	-6.71		-1.48	-3.57	-7.09	-1.19									-3.81	-1.65	-5.01	-2.57
10	-17.88	-1.97	-2.43	-4.03	-1.88				-4.03			-2.15	-5.99		-3.59	-1.01	-1.63	
11	-12.51												-1.85	-4.49	-2.44			

[a]Ref. 8.

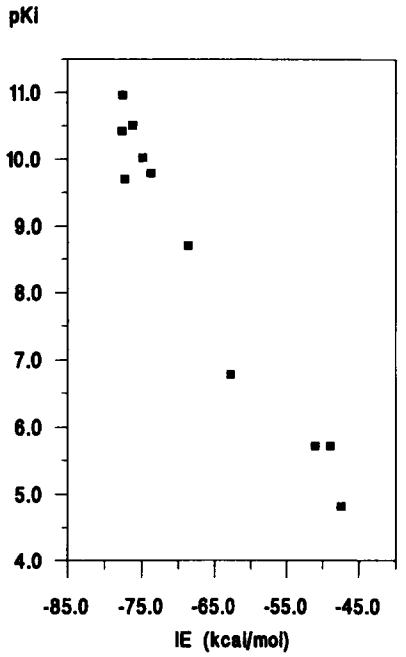

Figure 5. Correlation between the experimental pharmacological affinity data (pK_i) and the theoretical intermolecular interaction descriptor (IE). The linear regression equation is: $pK_i = -3.6171 (\pm 0.8335) - 0.1805 (\pm 0.0123)$ IE, $n = 11$, $r = 0.980$, $s = 0.476$.

run, the quaternary nitrogen atom of the ligands makes ionic interactions with the carboxylate of D307(147); moreover, for acetylcholine (**1**) and carbachol (**2**) the carbonylic oxygen atom of the agonists is constrained to make persistent H-bonding interactions with the alcoholic and the phenolic functions of T506(234) and Y616(506), respectively, according to site-directed mutagenesis experiment results;[14] furthermore, the carbonylic oxygen atom of oxotremorine-M (**3**) is constrained to interact with T506(234). N617(507) is never involved in H-bonding interactions with the agonists, consistently with site-directed mutagenesis results.[8] Furthermore, the agonists considered give persistent van der Waals' attractive interactions with Y308(148), consistently with the findings of Wess.[14] The agonist binding breaks the H-bonding interaction between N312(152) and W613(503) and the π–π stacking between W409(192) and W613(503) present in the free receptor structure and induces a shift of the side chain of W416(199) away from the binding site. Furthermore, Y308(148) gains a H-bonding interaction with Y616(506), S322(162) loses the H-bonding interaction with Y721(543) and R325(165) moves out of the highly conserved polar pocket, by losing the H-bond with N119(85).

As for the antagonist binding, in the dynamic model obtained, the protonated or quaternary nitrogen atom of the ligands makes permanent charge reinforced H-bonding or ionic interactions, respectively, with the carboxylate of D307(147) (Figs 6 and 7). The charge reinforced H-bonding interactions substantially influence the orientation and the interactions of the ligands during the MD simulation time period. In this respect, atropine (**5**) and scopolamine (**7**) give H-bonding interactions with S311(151), by utilizing the carbonyl function, while the corresponding quaternary analogs **6** and **8**, respectively, give only van der Waals' attractive interactions with this residue (Fig. 6). On the contrary, *N*-methylatropine (**6**) and NMS (**8**) give persistent H-bonding interactions with S314(154), by using both the carbonylic and the alcoholic oxygen atoms, while the protonated analogs **5** and **7** utilize only the alcoholic oxygen for interacting with this residue (Fig. 6). Also compound **9** makes a H-bond with S314(154) by means of the carbonylic oxygen atom. Moreover, compounds **6**, **8** and **9** give van der Waals' attractive interactions with D210(113), while the protonated antagonists **4**, **5**, **7**, **9** and **11** are more attracted by D307(147) and do not project toward D210(113), which is more buried than D307(147) (Figs 6 and 7).

All the antagonists considered, with the exception of compounds **10** and **11**, give persistent H-bonding interactions with S217(120); compounds **4–8** utilize the alcoholic oxygen atom while compound **9** interacts with the carbonylic function (Figs 6 and 7). These findings are consistent with site-directed mutagenesis experiments made on rat m3-muscarinic receptor.[14] Furthermore, Y707(529) gives π–π stacking or orthogonal σ–π interactions with one phenyl ring of the protonated compounds **4**, **5** and **7**, and van der Waals' attractive interactions with the cyclohexyl ring of compound **10**. On the contrary, this residue gives van der Waals' attractive interactions with the ring which contains the quaternary nitrogen atom of the antagonists **6**, **8** and **9** (Figs 6 and 7).

During the MD simulation time period, pirenzepine (**11**) showed a binding mechanism substantially different with respect to that of the other ligands. Consistently with the pharmacological affinity of this M1-selective antagonist, the IE of the minimized average pirenzepine–receptor complex is the less favoured in the series of the antagonists considered. In general, we have observed that, although each antagonist binds to the receptor in a different manner with respect to the others, in all the antagonist-bound structures obtained the conformational behaviour of the amino acids of helices 4–6 (which belong to the agonist binding site) is similar to that of the free average structure of the receptor; consequently, also the pattern of the H-bonding interactions involving the highly conserved polar amino acids [N119(85), D210(113), N317(157), R325(165) and Y721(543)] is mainly conserved in the average arrangement of the free receptor form. This may be related to the fact that the antagonist binding site is constituted by the amino acids of helices 1–3 and 7.

Concluding remarks

The results of this study generalize and support the mechanistic hypothesis previously presented.[7] In fact, the antagonists considered substantially preserve the average topography of the H-bonding interactions which involve, in the free receptor form, the amino acids of the highly conserved polar pocket lying near the cytosolic side and formed by N119(85), D210(113), R325(165), N717(539) and Y721(721). To the contrary, the agonists induce a rearrangement of the highly conserved polar pocket characterized also by the 'shift out' of R325(165) which lies near the cytosolic side notwithstanding the agonist binding occurs about 10 Å below the extracytosolic extremity of the receptor.

The consistency reached between the time-dependent structural rearrangement of the transmembrane seven-helix-bundle models obtained and the experimental pharmacological efficacies of the ligands constitutes a good validation of the 3-D models proposed. Further validation comes from the good QSAR models obtained by correlating the theoretical intermolecular interaction descriptor IE with the pharmacological affinities of the ligands considered.

However, the theoretical models presented are working hypotheses, which, by making use of the reductionistic approach, simplify and translate the complex physical nature of the experimental data into an appropriate formal chemical language. Their degree of realism is local and based on their internal consistency, which is better achieved within a comparative context.

Experimental

3-D Model building of the receptor and docking experiments

The building of the m3 input structure has been described in detail in our previous papers.[7,15] The m3 input structure was energy-minimized and then subjected to Molecular Dynamics. The structure averaged over the last 100 ps time period of each MD simulation was then minimized.

The input structures of the ligand–receptor complexes were obtained by docking each ligand in the minimized average structure of its target receptor. The complexes were energy-minimized. Minimizations were repeated several times, with different initial orientations of both the ligand and the receptor side chains in order to optimize the interactions known to be important by site-directed mutagenesis experiments.[14] It is worth noting that the analysis of site-specific mutagenesis experiments in structural terms, without a high resolution X-ray structure of the protein, is subjected to many un-

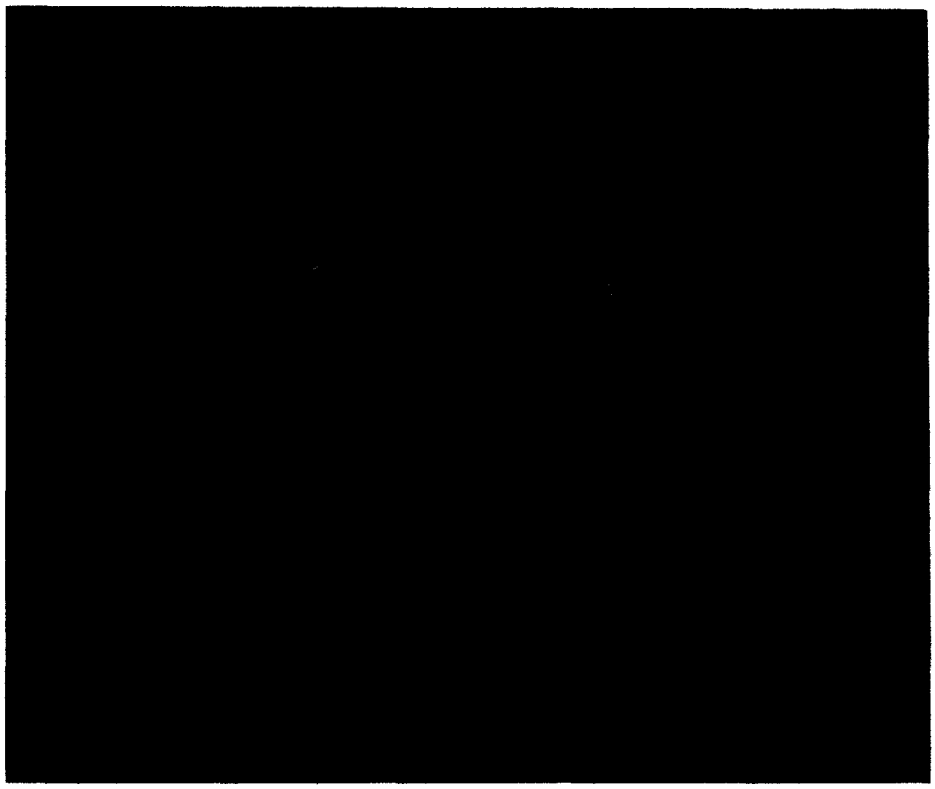

Figure 6. Details of the interaction between the antagonists NMS (top, left side), *N*-methylatropine (top, right side), scopolamine (bottom, left side), atropine (bottom, right side) and selected m3-receptor amino acid side chains. The amino acids are labelled according to the arbitrary numbering.

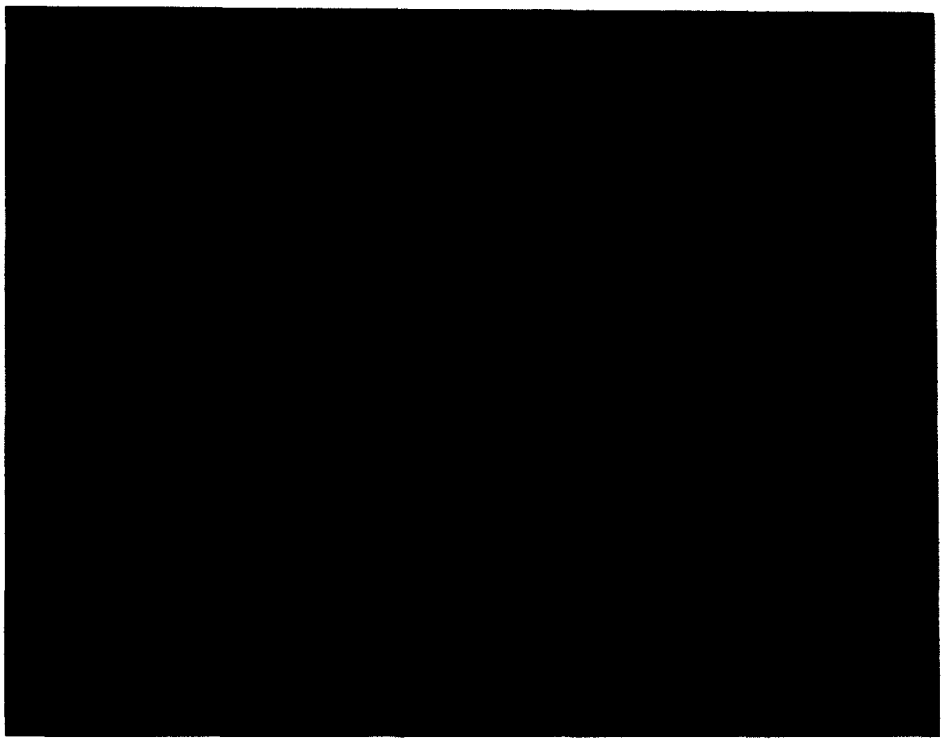

Figure 7. Details of the interactions between the antagonists (–)-QNB (top, left side), 4-DAMP (top, right side), triexylphenidyl (bottom, left side), pirenzepine (bottom, right side) and selected m3-receptor amino acid side chains. The amino acids are labelled according to the arbitrary numbering.

certainties; in this respect, we consider the docking strategy adopted in our study one of many possible.

The docking criteria were chosen according to the results of site-directed mutagenesis experiments which suggested that the amino functions of agonists and antagonists are bound in much the same way, but that the other molecular moieties recognize and bind different loci of the receptor. In particular, these experiments suggested that antagonists and agonists bind into different pockets formed by helices 1–3 and 7 and 3–6, respectively.[14] Apparently in contrast with these results Blüml *et al.* presented a work in which the N617(507) residue in the rat m3 sequence was replaced by alanine, serine and aspartic acid.[8] Radioligand binding studies with transfected COS-7 cells showed that the asparagine present in the TM 6 of all muscarinic receptors is not critical for acetylcholine and carbachol binding and for agonist-induced receptor activation, but plays a key role in the binding of certain subclasses of muscarinic antagonists. In fact, all three mutations led to dramatic reductions (235–28,300-fold) in binding affinities of the atropine-like agents and pirenzepine.[8] The authors said that it remains unclear at the present whether the Asn side chain directly interacts with distinct functional groups on the antagonist molecules or whether it only stabilizes a receptor conformation required for the high-affinity antagonist binding.[8,16]

We have observed that the binding affinities of the antagonists tested by Blüml *et al.*[8] for the three mutants are linearly correlated with a slope close to unity. These linear relationships may indicate that the effect of that mutation on the binding affinities does not depend on the chemical nature of the mutant residue. On the basis of these considerations it may be hypothesized that N617(507) may be not directly involved in the antagonist binding but that its mutation may cause a structural change in the receptor which reduces the affinity of some tested antagonists with respect to the wild type. Consistent with this hypothesis, in the previous study[7] we found that N617(507) lies in a position critical for the receptor structure; in fact we observed that the average minimized structures of the three mutant receptors N617(507) → A, N617(507) → S and N617(507) → D show seven-helix-bundle arrangements different with respect to the wild type (rms deviations of the backbone α-carbon atoms with respect to the wild type were 2.11 Å, 2.88 Å and 3.48 Å, respectively).[7] Moreover, consistent with the findings that the mutation of N617(507) into a serine constitutively activates the m3-muscarinic receptor,[8] we found that, notwithstanding N617(507) is near the extracytosolic side, this mutation induces a structural change which propagates towards the highly conserved polar pocket, lying near the cytosolic side.

According to site-directed mutagenesis experiments,[14] the charge reinforced H-bonding or the ionic interaction between the protonated or the quaternary nitrogen atom, respectively, of the muscarinic ligands and the carboxylate side chain of D307(147) were primarily optimized. Furthermore, additional interactions optimized were: 1) for the agonists carbachol and acetylcholine, the H-bonding interaction between the carbonylic oxygen atom of the ligands and both T506(234) and Y616(506); 2) for the agonist oxotremorine-M, the H-bonding interaction between the carbonylic oxygen atom of the ligand and T506(234); and 3) for the antagonists, the van der Waals' attractive interactions between the ligands and some amino acids of helices 1–3, and 7.

The minimized complexes obtained were subjected to the MD runs. All the atoms of both the ligand and the receptor were allowed to move during minimization and the MD simulation. Distance constraints were applied during the MD runs between the carbonylic oxygen atom of acetylcholine and carbachol and both the alcoholic and the phenolic hydrogen atoms of T506(234) and Y616(506), according to site-directed mutagenesis experiment results,[14] and between the carbonylic oxygen atom of oxotremorine-M and T506(234). These constraints were applied in order to study the structural/dynamics effect of the agonist binding. The structures averaged over the last 100 ps time period of each MD simulation were then minimized.

Computational procedure

Modelling studies were performed with the molecular graphics package QUANTA (version 4.0).[17] Energy minimizations and MD simulations of the receptors and of the ligand–receptor complexes were achieved on a HP-720 workstation by means of the program CHARMm (version 22).[18]

Minimizations were carried out by using the conjugate gradient minimizer, until the r.m.s. gradient was less than 0.001 kcal mol^{-1} Å. A distance dependent dielectric term ($\varepsilon = 4r$) and a 12 Å non-bonded cut-off distance were chosen. The 'united atom approximation' was used for computational efficiency.[18]

The minimized coordinates of the receptors and of the complexes were then used as the starting point for a 150 ps MD run. The proteins and the complexes were thermalized to 300 K with 5 °C rise per 6000 steps by randomly assigning velocities from the Gaussian distribution. After heating, the system was allowed to equilibrate for 34 ps. Velocities were scaled by a single factor. The system was then subjected to 110 ps MD simulation at constant temperature (300 K). The results reported were collected every 0.5 ps from the last 100 ps trajectory. The lengths of the bonds involving hydrogen atoms were constrained according to the SHAKE algorithm,[19] allowing an integration time step of 0.001 ps. The α-helices conformation was preserved by using the NOE constraint with a scaling factor of 10. These constraints were applied between the backbone oxygen atoms of residue i and the backbone nitrogen atoms of residue i + 4, excluding the prolines and R325(165) (it lies at the boundary between the TM3 and the second cytosolic loop). Integration of Newton's

equations of motion was done by using the Verlet algorithm.[20] The plots of the potential energy vs the equilibrated time period of the molecular dynamic simulations of four ligand–receptor complexes are reported in Figures 8 and 9.

The interaction energies (IE) of the ligand–receptor average minimized complexes were computed according to the following formula: $IE = E_{COMPLEX} - E_{REC} - E_{LIG}$, where $E_{COMPLEX}$ is the energy of the ligand–receptor complex, E_{REC} and E_{LIG} are the energies of the receptor and of the ligand, respectively, in the complex. The charge distributions of the ligands in their protonated or quaternary forms were obtained in the AM1 framework.[21]

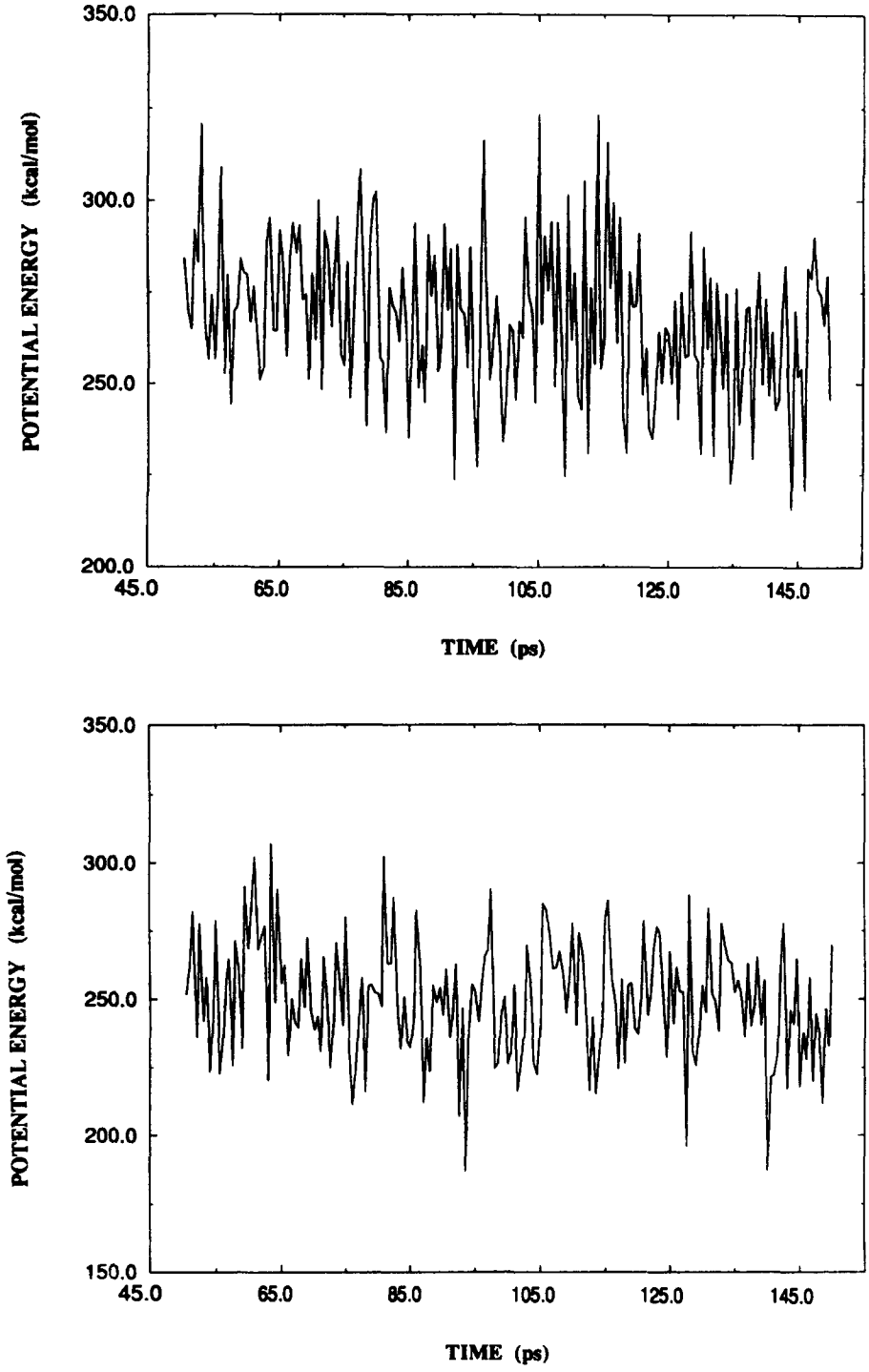

Figure 8. Potential energy (kcal mol^{-1}) vs the equilibrated time period (ps) of the molecular dynamics simulation for the complexes of the m3-muscarinic receptor with the antagonists atropine (top) and NMS (bottom).

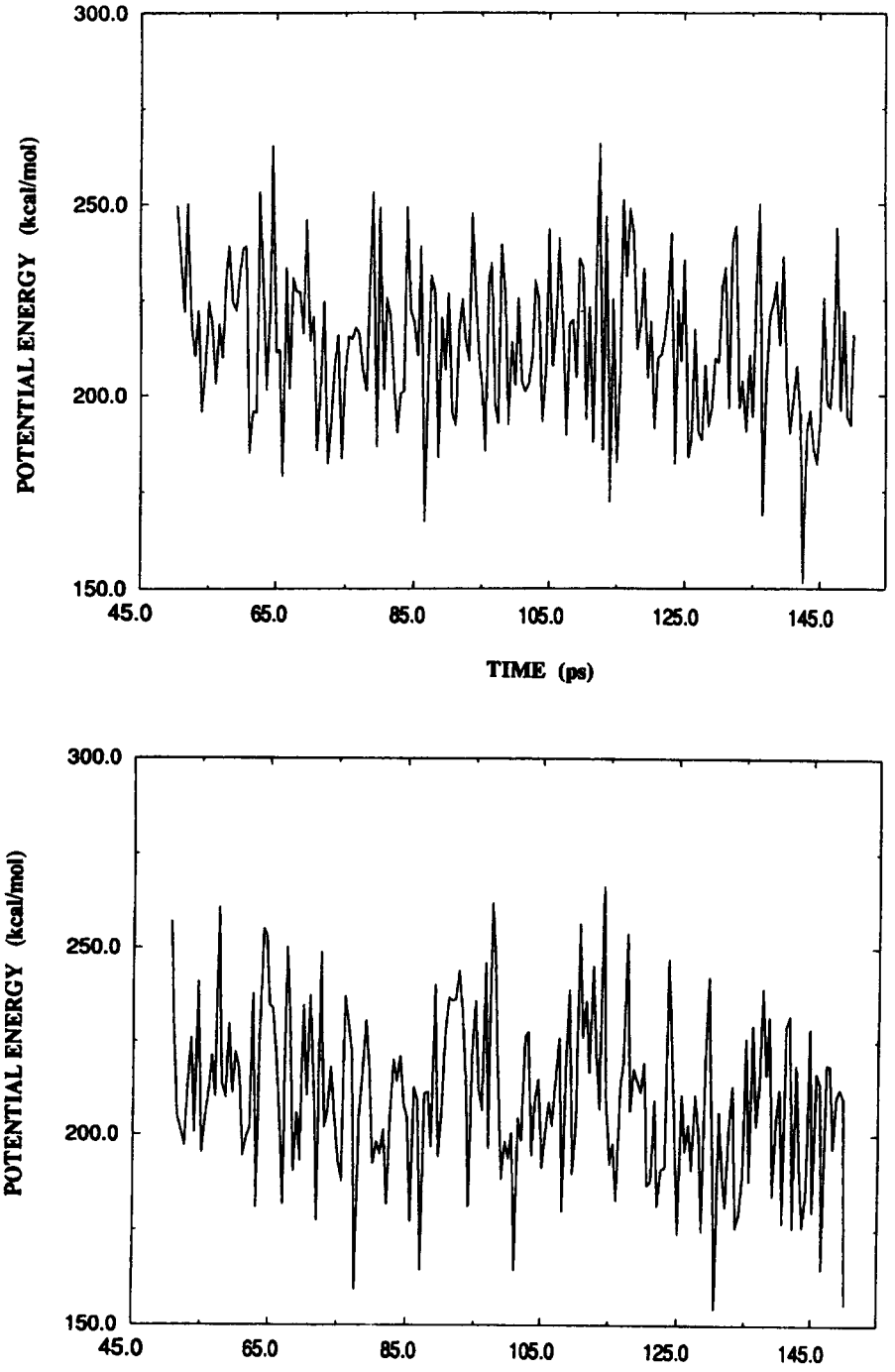

Figure 9. Potential energy (kcal mol^{-1}) vs the equilibrated time period (ps) of the molecular dynamics simulation for complexes of the m3-muscarinic receptor with the agonists acetylcholine (top) and carbachol (bottom).

Acknowledgements

Financial support from the Consiglio Nazionale delle Ricerche (Roma) and Ministero dell' Università e della Ricerca Scientifica (funds 40%) is acknowledged.

References

1. Timms, D.; Wilkinson, A. J.; Kelly, D. R.; Broadley, K. J.; Davies, R. H. *Int. J. Quantum Chem., Quantum Biol. Symp.* **1992**, *19*, 197.

2. Timms, D.; Wilkinson, A. J.; Kelly, D. R.; Broadley, K. J.; Davies, R. H. *Receptors and Channels* **1994**, *2*, 107.

3. Olivieira, L.; Paiva, C. M.; Sander, C.; Vriend, G. *Trends Pharmacol. Sci.* **1994**, *15*, 170.

4. Zhang, D.; Weinstein, H. *J. Med. Chem.* **1993**, *36*, 934.

5. Luo, X. C.; Zhang, D. Q.; Weinstein, H. *Protein Engineering* **1994**, *7*, 1441.

6. Kontoyianni, M.; Lybrand, T. P. *Med. Chem. Res.* **1993**, *3*, 407.

7. Fanelli, F.; Menziani, M. C.; De Benedetti, P. G. *Protein Engineering*, **1995**, *6*, 557.

8. Blüml, K.; Mutschler, E.; Wess, J. *J. Biol. Chem.* **1994**, *269*, 18870.

9. Franke, R. R.; Koning, B.; Sakmar, T. P.; Khorana, H. G.; Hofmann, K. P. *Science* **1990**, *250*, 123.

10. Zhu, S. Z.; Wang, S. Z.; Hu, J.; El-Fakahany, E. *Mol. Pharmacol.* **1994**, *45*, 517.

11. Ballesteros, J. A.; Weinstein, H. *Meth. Neurosci.* **1995**, *25*, 366.

12. Gilli, G.; Borea, P. A. *The Application of Charge Density Research to Chemistry and Drug Design*; Jeffrey, G. A.; Piniella, J. F., Eds; Plenum Press: New York, 1991; pp. 241–286.

(*Received in U.S.A.* 24 *April* 1995; *accepted* 3 *July* 1995)

13. Fanelli, F.; Menziani, M. C.; Carotti, A.; De Benedetti, P. G. *Bioorg. Med. Chem.* **1994**, *2*, 195.

14. Wess, J. *Life Sci.* **1993**, *53*, 1447.

15. Fanelli, F.; Menziani, M. C.; Cocchi, M.; De Benedetti, P. G. *J. Mol. Struct. (THEOCHEM)* **1995**, *333*, 49.

16. Wess, J.; Blin, N.; Mutschler, E.; Blüml, K. *Life Sci.* **1995**, *56*, 915.

17. QUANTA/CHARMm, 1990, Molecular Simulations, 200 Fifth Avenue, Waltham, MA 02254.

18. Brooks, B. R.; Bruccoleri, R. E.; Olafson, B. D.; States, D. J.; Swaminathan, S.; Karplus, M. *J. Comput. Chem.* **1983**, *4*, 187.

19. van Gunsteren, W. F.; Berendsen, J. C. *Mol. Phys.* **1987**, *34*, 1311.

20. Verlet, L. *Phys. Rev.* **1967**, 159, 98.

21. Dewar, M. J. S.; Zoebisch, E. G.; Healey, E. F.; Stewart, J. J. P. *J. Am. Chem. Soc.* **1985**, *107*, 3902.